Spectrochimica Acta Part A 75 (2010) 1108–1114

Contents lists available at ScienceDirect

Spectrochimica Acta Part A: Molecular and Biomolecular Spectroscopy

journal homepage: www.elsevier.com/locate/saa

DNA binding and photocleavage specificities of a group of tricationic metalloporphyrins

Ping Zhao [a,b], Jin-Wang Huang [a,*], Wen-Jie Mei [b], Juan He [b], Liang-Nian Ji [a]

[a] MOE Laboratory of Bioinorganic and Synthetic Chemistry, School of Chemistry and Chemical Engineering, Sun Yat-Sen University, No. 135, Xin Gang Xi Road, Guangzhou 510275, PR China
[b] School of Chemistry and Chemical Engineering, Guangdong Pharmaceutical University, Guangzhou 510275, PR China

ARTICLE INFO

Article history:
Received 15 September 2009
Received in revised form
21 December 2009
Accepted 22 December 2009

Keywords:
Metalloporphyrin
DNA binding
Steric hindrance
DNA photocleavage

ABSTRACT

The interactions of 5,10,15-tris(1-methylpyridinium-4-yl)-20-(4-hydroxyphenyl)porphyrinatozinc(II) Zn[TMPyHP]$^{3+}$ (**2**) along with Cu[TMPyHP]$^{3+}$ (**3**), Co[TMPyHP]$^{4+}$ (**4**), Mn[TMPyHP]$^{4+}$ (**5**) and the free base porphyrin H_2[TMPyHP]$^{3+}$ (**1**) with duplex DNA have been studied by using a combination of absorption, fluorescence titration, surface-enhanced Raman spectroscopy (SERS), induced circular dichroism (ICD) spectroscopy, thermal DNA denaturation, viscosity measurements as well as gel electrophoresis experiment. Their binding modes and intrinsic binding constants (K_b) to calf DNA (CT DNA) were comparatively studied and were found significantly influenced by different metals coordinated with the porphyrin plane. Except **3**, which has four-coordination structure at the metal, all the metal derivatives showed non-intercalative DNA-binding mode and lower K_b than the free base porphyrin **1**, most probably due to the steric hindrance results from the axial ligands of the inserted metals which are five or six-coordination structures. Meanwhile, the insertion of metals into cationic porphyrin greatly removed the self-aggregation of the metal-free porphyrins, and thus fully enhanced the singlet oxygen ($^1O_2$) productivities in the DNA photocleavage experiments. Therefore, these metalloporphyrins have comparable DNA cleavage ability with the free base porphyrin.

1. Introduction

The design of small complexes that bind and react with DNA becomes important as we begin to delineate the expression of genetic information on a molecular level. A complete understanding of how to target DNA sites with specificity will lead not only to novel chemotherapeutics but also to a greatly expanded ability for chemists to probe DNA and to develop highly sensitive diagnostic agents [1–5]. Transition-metal complexes are being used at the forefront of many of these efforts. Stable, inert, and water-soluble complexes containing spectroscopically active metal centers are extremely valuable in the researches of biological systems. More recently, such metal complexes have been applied to probe both structural and functional aspects of nucleic acid chemistry [6–8].

One of the most versatile metal complexes for nucleic acid research is the metalloporphyrins. A number of metalloporphyrins have been used in various fields of DNA study such as DNA breaks [9,10], probes of DNA structure [11], enhancement of restriction enzyme activity [12] and photoactive insecticides [13]. Most especially, the cationic metalloporphyrin derivatives of Cu(II), Co(III), Ni(II) and Mn(III) with tetra-kis(1-methylpyridinium-4-yl)porphyrin (H_2TMPyP)$^{4+}$ have been intensely investigated in the past [14–18]. Nevertheless, so far no studies have focused on the role unsymmetrical cationic metalloporphyrins played in the DNA research.

We recently reported the synthesis and the DNA binding and photocleavage properties of a series of metal-free tricationic pyridium porphyrins with different peripheral active groups [19–22]. It was found that, among them, only the tricationic pyridium porphyrin appending a hydroxyphenyl group, H_2[TMPyHP]$^{3+}$, could intercalate into DNA base pairs, cleave DNA efficiently and hence may be a candidate for PDT instead of (H_2TMPyP)$^{4+}$. In this paper, we synthesized the zinc(II) (**2**), copper(II) (**3**), cobalt(III) (**4**), manganese(III) (**5**) (Fig. 1) complexes of H_2[TMPyHP]$^{3+}$ (**1**), and studied their binding properties with CT DNA. Meanwhile, the photocleavage of pBR322 plasmid DNA by these porphyrins were also comparatively investigated.

2. Experimental

2.1. Materials and chemicals

The metalloporphyrin derivatives were prepared by mixing the free base porphyrin **1** with corresponding acetate salts in the dark

* Corresponding author. Tel.: +86 20 84113317; fax: +86 20 84112245.
E-mail address: ceshjw@163.com (J.-W. Huang).

1386-1425/$ – see front matter © 2010 Elsevier B.V. All rights reserved.
doi:10.1016/j.saa.2009.12.065

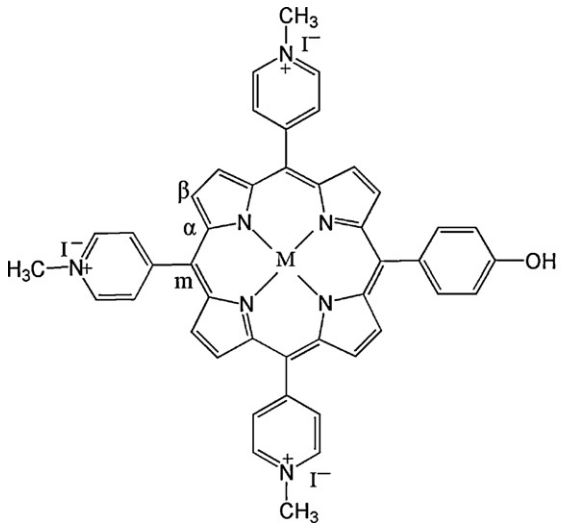

No.	M^{n+}	Short Formula
1	$2H^+$	H_2TMPyHP
2	Zn^{2+}	ZnTMPyHP
3	Cu^{2+}	CuTMPyHP
4	Co^{3+}	CoCl(TMPyHP)
5	Mn^{3+}	MnCl(TMPyHP)

Fig. 1. The molecular structures of porphyrins **1–5**.

[21–23]. The formation of the metalloporphyrins was confirmed by the measurement of UV–vis absorption spectra.

The spectroscopic results obtained from 5,10,15-tris(1-methylpyridinium-4-yl)-20-(4-hydroxyphenyl)porphyrinatozinc (**2**): ^{1}H NMR (300 MHz, DMSO): chemical shift δ: 9.48(d, J = 5.94 Hz, 6H, 2, 6-pyridinium), 9.11(s, 4H, β-pyrrole), 9.07(s, 4H, β-pyrrole), 9.00(d, J = 5.51 Hz, 6H, 3,5-pyridinium), 8.02(d, J = 8.13 Hz, 2H, 2,6-phenyl), 7.26(d, J = 8.06 Hz, 2H, 3,5-phenyl), 4.73(s, 9H, N^+–Me), 3.01(s, 1H, OH). ES-MS [EtOH, m/z]: 247 ($[M]^{3+}$). UV–vis (10 μM in Tris buffer), λ_{max}(nm) ($\log\varepsilon$): 425(4.9), 563(3.4), 583(3.3).

The spectroscopic results obtained from 5,10,15-tris(1-methylpyridinium-4-yl)-20-(4-hydroxyphenyl)porphyrinatocopper (**3**): ES-MS [EtOH, m/z]: 246 ($[M]^{3+}$). UV–vis (10 μM in Tris buffer), λ_{max}(nm) ($\log\varepsilon$): 426(4.8), 560(3.2), 584(3.1).

The spectroscopic results obtained from 5,10,15-tris(1-methylpyridinium-4-yl)-20-(4-hydroxyphenyl)porphyrinatocobalt (**4**). ES-MS [EtOH, m/z]: 245 ($[M]^{3+}$). UV–vis (10 μM in Tris buffer), λ_{max}(nm) ($\log\varepsilon$): 425(5.0), 563(3.4).

The spectroscopic results obtained from 5,10,15-tris(1-methylpyridinium-4-yl)-20-(4-hydroxyphenyl)porphyrinatomanganese (**5**). ES-MS [EtOH, m/z]: 243 ($[M]^{3+}$). UV–vis (10 μM in Tris buffer), λ_{max}(nm) ($\log\varepsilon$): 425(4.8), 561(3.3), 585(3.1).

Buffer A (5 mM Tris–HCl, 50 mM NaCl, pH 7.2, Tris = Tris (hydroxymethyl)aminomethane) solution was used in all the experiments except for the thermal denaturation studies in which buffer B (1.5 mM Na_2HPO_4, 0.5 mM NaH_2PO_4, 0.25 mM Na_2H_2EDTA (H_4EDTA = N,N′-ethane-1,2-diylbis[N-(carboxymethyl)glycine]), pH 7.0) was used. CT DNA and pBR322 supercoiled plasmid DNA were obtained from the Sigma Company. A solution of CT DNA in the buffer A gave a ratio of UV absorbance at 260 and 280 nm of 1.85:1, indicating that the DNA was sufficiently free of protein. The DNA concentration per nucleotide was determined by absorption spectroscopy using the molar absorption coefficient (6600 M^{-1} cm^{-1}) at 260 nm [24]. Unless otherwise stated, reagents were commercially available and of analytical grade.

2.2. Measurements

Electrospray mass spectra (ES-MS) were recorded on a LCQ DECA XP liquid chromatography–mass spectrometry (Thremo, USA). ^{1}H NMR spectra were recorded on a Mercury-Plus 300 Nuclear Magnetic Resonance Spectrometer (Varian, USA). UV–vis spectra were recorded on a PerkinElmer-Lambda-850 spectrophotometer. Fluorescence spectra were recorded on a PerkinElmer L55 spectrofluorophotometer at room temperature. SERS spectra were carried out on an inVia Laser Micro-Raman Spectrometer of Renishaw, with a power of 20 mW at the samples. ICD Spectra were recorded on a JASCO-J810 spectrometer. Thermal denaturation studies were carried out with a PerkinElmer-Lambda-850 spectrophotometer equipped with a Peltier temperature-controlling programmer (±0.1 °C). The melting curves were obtained by measuring the absorbance at 260 nm for solutions of CT DNA (100 μM) in the absence and presence of the porphyrin compound (10 μM) as a function of the temperature. The temperature was scanned from 30 to 90 °C at a speed of 1 °C min^{-1}. The melting temperature (T_m) was taken as the mid-point of the hyperchromic transition.

In the SERS experiment, Ag colloids were prepared by reducing $AgNO_3$ with EDTA according to the reported method [25]. The Ag colloid/compound (or Ag colloid/DNA) SERS-active systems were prepared by mixing equal volume of the porphyrin (or DNA) solution with the Ag colloid in buffer A to obtain the desired porphyrin or DNA concentrations. In the porphyrin/DNA complex experiments, the solution of DNA was mixed with the porphyrin solution at a DNA/porphyrin ratio of 30:1, then an equal volume of the mixed solution was fully mixed with the Ag colloid, and the spectrum was immediately measured at room temperature. The final concentrations of porphyrins and DNA in all of the SERS-active systems were 5 and 150 μM, respectively.

For the gel electrophoresis experiment, pBR322 supercoiled plasmid DNA (0.1 μg) was treated with the porphyrin compound in buffer C (50 mM Tris–HCl, 18 mM NaCl, pH 7.2), and the solution was then irradiated at room temperature with a high-pressure mercury lamp/monochromator assembly. The samples were analyzed by electrophoresis for 1 h at 120 V in Tris–acetate buffer containing 1% agarose gel. The gel was stained with 1 μg ml^{-1} 3,8-diamino-5-ethyl-6-phenylphenanthridinium bromide (EB) and photographed under UV light.

3. Results and discussion

3.1. DNA-binding studies

3.1.1. Absorption titrations

One of the most common techniques in DNA-binding studies of porphyrins is electronic absorption spectroscopy. The magnitude of spectral perturbation is an evidence for DNA-binding [9,14,15]. As is well known, intercalation of porphyrin into DNA base pairs is characterized by a bathochromism (>8 nm) and hypochromism (up

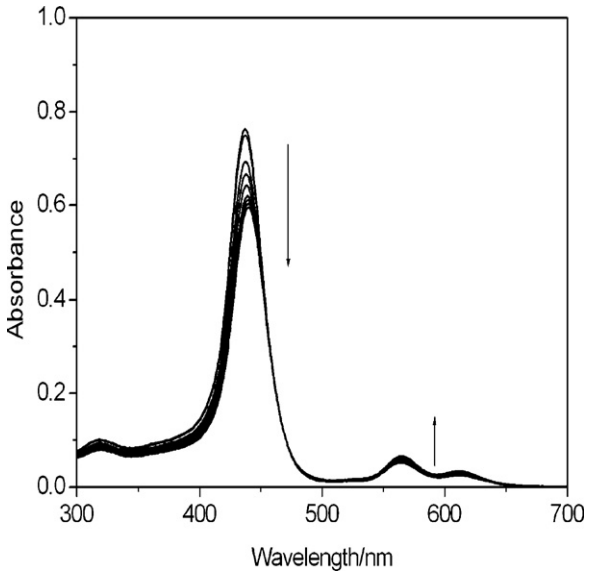

Fig. 2. Absorption spectra of **2** in buffer A at 25 °C in the presence of increasing amounts of CT DNA. [Por] = 10 μM. Arrows indicate the change in absorbance upon increasing the DNA concentration.

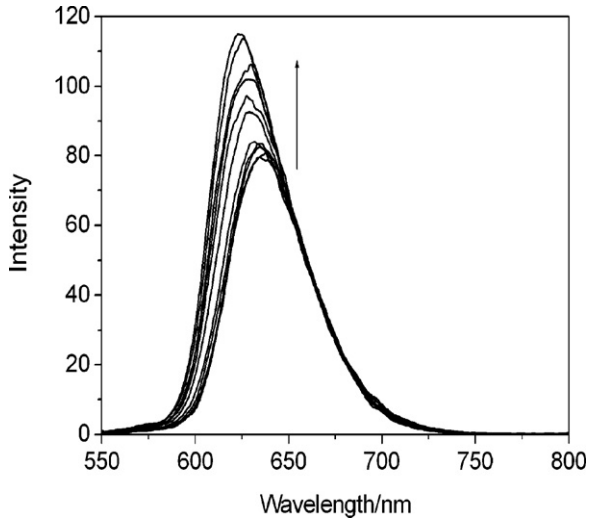

Fig. 3. Emission spectra for **2** in the absence and presence of CT DNA, in buffer A. Arrows show the intensity change upon increasing DNA concentrations. [Por] = 10 μM; λ_{ex} = 449 nm.

to 40%) in the Soret band of UV–vis spectra; groove binding mode shows no (or minor) and outside binding mode exhibits moderate change in UV–vis spectra of porphyrins [9,14,15,19–22]. The DNA titration absorption spectroscopy of porphyrin **2** is shown in Fig. 2 and analogous spectra were obtained in the case of other porphyrins (see supporting materials). All physical data about the change of porphyrins' absorption spectra in the presence of increasing amounts of CT DNA are collected in Table 1. With increasing CT DNA concentration, different extents of bathochromism and hypochromism are observed in the Soret bands for all the metalloporphyrins, indicating different DNA-binding modes of them. The large bathochromism and hypochromism of porphyrin **3** (9 nm and 45.9%) indicate that it may intercalate into DNA, which is similar to the DNA-binding behavior of its free base porphyrin ligand **1**. However, the moderate or minor changes in the absorbance spectra of **2**, **4** and **5** suggest that these three metalloporphyrins may employ non-intercalative binding modes.

In order to compare the affinities of the porphyrins bound to CT DNA quantitatively, the intrinsic binding constants K_b were measured by monitoring the changes of absorbance in the Soret band with increasing concentration of CT DNA using the following equation [15]:

$$\frac{[DNA]}{(\varepsilon_a - \varepsilon_b)} = \frac{[DNA]}{(\varepsilon_a - \varepsilon_f)} + \frac{1}{K_b(\varepsilon_b - \varepsilon_f)}$$

where [DNA] is the concentration of DNA in base pairs, ε_a, ε_f and ε_b correspond to the apparent absorption coefficient A_{obsd}/[Por] ([Por], the concentration of porphyrin), the extinction coefficient for the free porphyrin complex and the extinction coefficient for the porphyrin complex in the fully bound form, respectively. From the plot of [DNA]/($\varepsilon_a - \varepsilon_f$) versus [DNA], K_b of the porphyrin compounds were calculated and the results were listed in Table 1, too.

Table 1
Physical data of porphyrins binding with CT DNA.

Porphyrin	UV titration		ICD signal		ΔT_m (°C)	K_b
	Δλ (nm)	H%				
1	10	47.5		–	9.1	4.9×10^5
2	3	29.8	+		3.4	1.8×10^5
3	9	45.9		–	7.8	4.1×10^5
4	5	30.8	+	–	4.6	2.4×10^5
5	6	36.8	+		5.0	3.3×10^5

From Table 1, we can find that the values of K_b have strict relationship with respect to the coordinated metal in the porphyrin core. The free base porphyrin **1** and the metalloporphyrin **3** with Cu(II) in the centre have larger K_b than the porphyrins coordinated with Zn(II), Co(III), Mn(III). From the spectrophotometric titrations of the porphyrin solutions, **1** and **3** were proved to employ intercalative (which is more advantageous) modes when bind with DNA while porphyrins **2**, **4** and **5** via non-intercalative modes. Thus, we suppose that the different K_b may mainly result from the distinct DNA-binding modes.

3.1.2. Fluorescence titration

Fluorescence titration experiments in the presence of CT DNA were performed. In our previous study, the fluorescence emission of the free base porphyrin **1** decreased remarkably at the initial stage of DNA titration and then increased significantly at higher concentrations of DNA [19,20]. It could be ascribed to self-stacking of the porphyrin molecules along the DNA surface, and is widely accepted as a criterion for intercalation [17,19]. Large increases in intensities of fluorescence emission are depicted for porphyrin **2** in the presence of increasing DNA amount (Fig. 3), which implies that Zn(II) porphyrin can be protected by the hydrophobic environment inside the DNA helix efficiently. Since no obvious decease of fluorescence emission for porphyrin **2** was found at any stage of DNA titration, non-intercalative DNA-binding mode maybe employed by the Zn(II) porphyrin.

Cu(II), Co(III) and Mn(III) porphyrins **3**, **4** and **5** show negligible luminescence in buffer A and neglectable changes were found with the addition of DNA. For complexes exhibiting a weak or no emission intensity in the presence of DNA, competitive binding to DNA with EB provides rich information regarding the nature of DNA binding [26,27]. EB emits intense fluorescence in the presence of DNA, due to its strong intercalation between the adjacent DNA base pairs of DNA [28]. The emission spectra of DNA-bound EB solution significantly quenched with increasing concentrations of the metalloporphyrins and the quenching plots were given in Fig. 4. From Fig. 4, we can find that porphyrin **3** could quench the emission of EB to a greater extent than porphyrin **4** and **5**. It is widely accepted that the emission decreases of DNA-bound EB solution results from the extrusion of EB from DNA duplex structures. Generally, the extrusion of EB occurs by replacing of other intercalating compounds, or

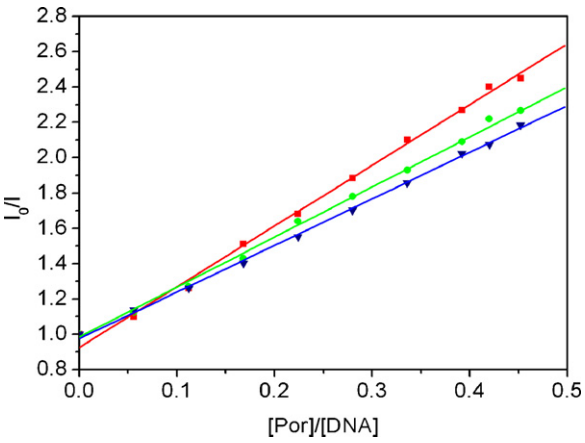

Fig. 4. Fluorescence quenching plots of DNA-bound EB by **3** (■), **4** (●) and **5** (▼) in buffer A. [DNA] = 100 μM, [EB] = 16.0 μM, and λ_{ex} = 537 nm.

it can occur indirectly by changing the DNA conformation as a result of binding of non-intercalating compounds [26–28]. The quenching extent of direct EB replacement is always larger than the indirect DNA change. Thus, it is suggested that the Cu(II) porphyrin **3** intercalate into DNA duplexes while the Co(III) and Mn(III) porphyrins **4** and **5** may change the conformation of DNA when bound with it.

3.1.3. SERS investigation

SERS is a powerful tool for the study of the interactions of drugs, especially fluorescence molecules, with biomacromolecules at very low concentrations. The metal colloids can be adapted for the application in the study of biological objects, because they do not modify to a great extent the structures of biological molecules adsorbed on their surface [29]. To further prove the interactions of these metalloporphyrins with CT DNA, SERS spectra were measured.

The SERS spectra of the porphyrins in the absence and presence of CT DNA are shown in Fig. 5. Table 2 summarized the main SERS bands of the porphyrins and their assignments. Fig. 5 also exhibited the SERS spectrum of free CT DNA. It is found that no substantial SERS signal is given by free CT DNA, since the Ag colloids have negative charges on their surface, which repulses the adsorption of negative-charged DNA molecules [30].

Curves 1–5 and 1′–5′ in Fig. 5 show the SERS spectra of the porphyrins in the absence and presence of DNA, respectively. In the presence of DNA, most bands of the porphyrin compounds disappear, indicating that the interactions of porphyrins with DNA can largely reduce the amount of porphyrins adsorbed on Ag colloids [31]. Especially, the disappearance of the band at 330 cm^{-1} which is mainly assigned to the bending vibration and is the marker band of Por ring doubtlessly proves the vanishment of porphyrin molecules surrounding Ag colloids after the interaction between metalloporphyrins and DNA [31–33]. The vanishment of bands centered at 411, 814, 965, 1001, 1098, 1141 nm also indicates the porphyrins are protected by DNA from adsorbing on Ag particles.

Table 2
Raman frequencies and assignments for porphyrins.[a]

Raman shift (cm^{-1})	Assignments[b]
330	δ(por)
411	δ(por) + ν(Ag–N)
814	pyr ν(N^+–CH_3), δ_s(por)
965	ν(C_α–C_β)
1001	ν(C_m–C_α)
1098	δ_s(C_β–H)
1191	δ(pyr), ν(N^+–CH_3)
1214	δ(pyr), ν(C_α–N)
1242	ν(C_m–pyr)
1337	ν_s(N–C_α)
1141	ν(C_α–N)
1554	ν(C_β–C_β)

[a] Band assignments are according to Refs. [29–34].
[b] *Abbreviations*: ν, stretching mode; δ, bending mode; *s*, symmetric mode; pyr, *N*-methylpyridinium; por, porphyrin core.

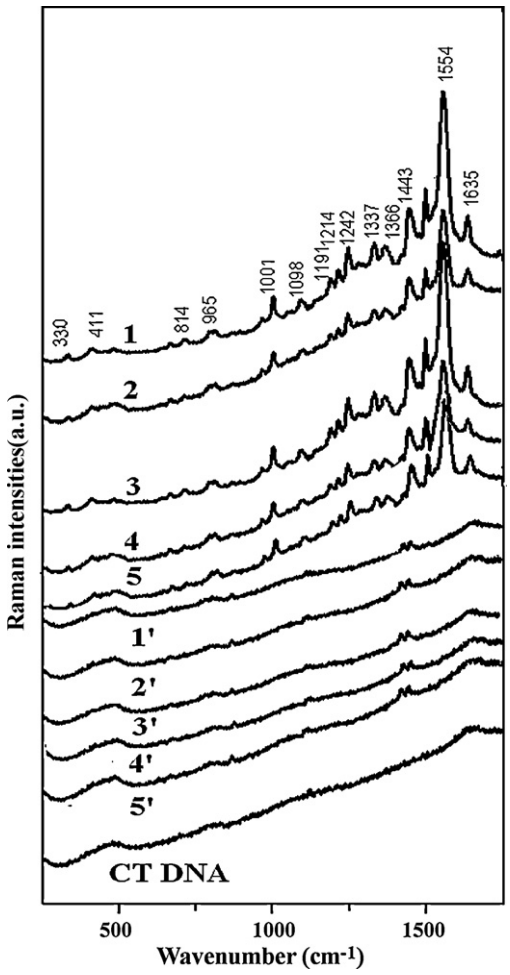

Fig. 5. SERS spectra (250–3000 cm^{-1}) of CT DNA and porphyrins in the absence (1–5) and presence (1′–5′) of CT DNA. (1), (2), (3), (4), (5) for free porphyrins **1**–**5**, respectively; (1′), (2′), (3′), (4′), (5′) for DNA complexes with **1**–**5**, respectively. [DNA]/[Por] = 30:1.

Moreover, the spectral changes confirm that the cationic porphyrins efficiently bind to DNA even in Ag sols. In this medium, the preference of cationic porphyrins for polyanionic DNA prevails over negatively charged Ag nanoparticles. This also reveals the high binding affinities between the cationic drugs and DNA [34].

3.1.4. ICD studies

The ICD spectrum experiment may be one of the most direct means in examining the binding modes of the porphyrin compounds to DNA. None of these compounds as well as DNA by themselves displays any CD spectra signal in the visible region, but ICD spectra were observed in the Soret band of these compounds in the presence of DNA due to the interaction between the transition moments of the achiral porphyrin and chirally arranged DNA base transitions. The sign of the ICD spectrum of DNA in the Soret region can be used as a sensitive signature for the binding modes of porphyrins to DNA: a positively ICD band is indicative of external (minor groove) binding, a negatively ICD band is produced upon intercalation and a conservative bisignal ICD band is the characteristic of outside binding [14,15].

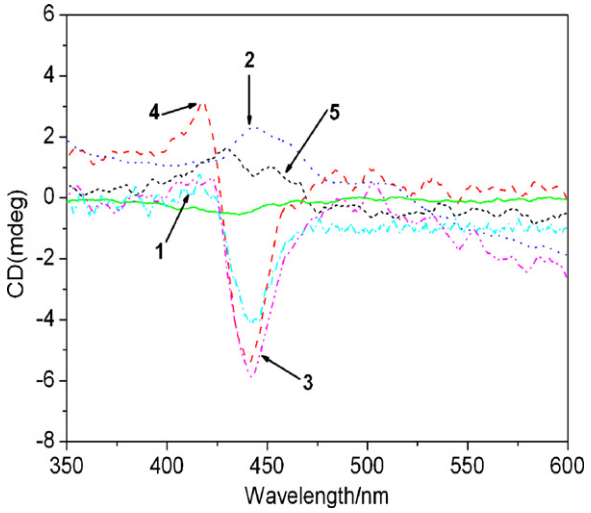

Fig. 6. ICD spectra of porphyrins in the absence (dot line) and presence (solid line) of CT DNA in buffer A. [Por] = 10 μM; [Por]/[DNA] = 0.1.

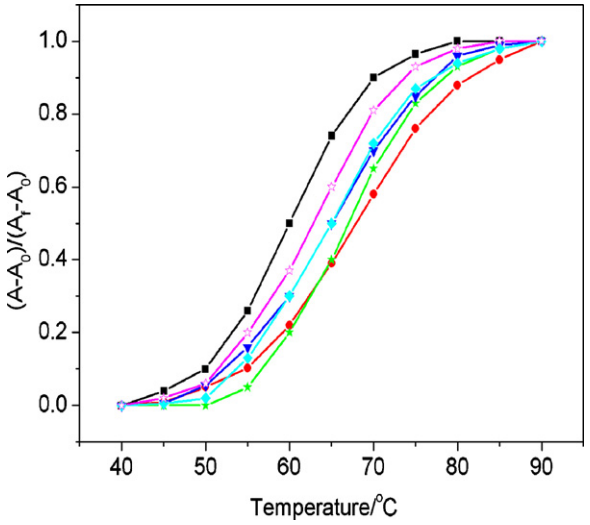

Fig. 7. Melting curves of CT DNA at 260 nm in the absence (■) and the presence of **1** (●), **2** (☆), **3** (★), **4** (▼) and **5** (◆), in buffer B. [Por] = 10 μM; [DNA] = 100 μM.

Fig. 6 and Table 1 give the results of ICD study which was also carried out to investigate the binding modes of the cationic porphyrins. As shown in Fig. 6, free base porphyrin **1** shows strong negative peak centered at ca. 445 nm upon binding to CT DNA, indicating that it is an excellent DNA intercalator. Similar negative signal was observed in the case of its copper derivative **3**, suggesting that the coordination of Cu(II) in the porphyrin core does not influence the intercalation of porphyrin plane into the DNA bases. As to the Zn(II)–, Mn(III)– complexes of **1**, positive CD spectra in the range of 410–430 nm were observed, which is consistent with groove binding mode. As to Co(II) complexes **4**, in the presence of DNA, both positive and negative ICD spectra appeared, indicating an outside binding mode. The result of ICD experiment unambiguously proves the binding modes we proposed in the absorption and fluorescence experiments.

From the experimental results, we can find that Cu(II) complexes of free base porphyrin **1** can still intercalate into DNA bases while Zn(II)–, Co(III), Mn(III) complexes can only employ outside or groove binding modes when interact with DNA. This may result from that, similar to the case of $(H_2TMPyP)^{4+}$, when inserts in the porphyrin core of **1**, Cu(II) has four-coordination structure and no extra ligands on the axial position of porphyrin plane; Zn(II) has five-coordination structure with a water molecule as the axial ligand; Co(III), Mn(III) have six-coordination structure with a water molecule and a Cl atom as axial ligands [7,14,15,17]. The axial ligands of these metalloporphyrins increase the steric hindrance of the porphyrin molecules and thus, only Cu(II) derivative, porphyrin **3**, is sterically appropriate to bind with DNA in intercalative mode while the metalloporphyrins **2**, **4** and **5** are not.

3.1.5. Thermal denaturation studies

The melting temperature (T_m) of DNA is sensitive to its double helix stability and the binding of compounds to DNA alters the T_m depending on the strength of interactions [14,15]. Therefore, it can be used as an indicator of binding properties of porphyrins to DNA and their binding strength. T_m will considerably increase when intercalation binding mode occurs [14,35].

The melting curves of CT DNA in the absence and presence of porphyrins are presented in Fig. 7. The T_m of CT DNA is $(61.1 \pm 0.2)^\circ$C in the absence of the porphyrins. When mixed with the porphyrins at a concentration ratio [Por]/[DNA] of 1:10, the observed melting temperatures of CT DNA increase to different degrees. The differences, designed as ΔT_m, are collected in Table 1. Here $\Delta T_m = T_m - T_m^0$, T_m and T_m^0 refer to the melting temperature of DNA in the presence and absence of porphyrins, respectively.

The large increases of T_m in the presence of **1** and **3** (ΔT_m = 9.1 and 7.8 °C, respectively) indicate that these two porphyrins interact with DNA in a typical intercalative mode and have strong DNA-binding affinities. The small increases of T_m in the presence of **2**, **4** and **5** (ΔT_m = 3.4, 4.6 and 5.0 °C, relatively) give us the information that these metalloporphyrins do not intercalate into DNA and have relatively weaker DNA-binding affinity than the free base porphyrin and its Cu(II) complex. These results are in good agreement with the experiments above.

3.1.6. Viscosity measurement

In the absence of X-ray structural data, viscosity measurement is regarded as the least ambiguous and the most critical test of a DNA-binding model in solution and provides strong arguments for intercalative DNA-binding mode. Intercalative mode is expected to lengthen the DNA helix as the base pairs are pushed apart to accommodate the bound ligand, leading to an increase in the DNA viscosity. In contrast, a partial, non-classical intercalation of ligand could bend (or kink) the DNA helix and reduce its effective length and, concomitantly, its viscosity. When outside binding occurs, the viscosity of DNA would not change basically [36].

Fig. 8 shows the effects of porphyrins on the viscosity of rod like DNA, which is very sensitive to the binding modes of the ligands. On increasing the amounts of **1** and **3**, the relative viscosity of DNA increases steadily. However, the increases of porphyrins **2**, **4** and **5** have no obvious effect on the relative viscosity of DNA. The viscosity results show that the free base porphyrin **1** and its Cu(II) derivative intercalate between the base pairs of DNA, while the its Zn(II)–, Co(III)–, Mn(III) complexes bind to DNA in outside or groove binding mode. The distinct results of viscosity experiment convincingly prove the conclusion above.

3.2. DNA photocleavage experiment

The cleavage reaction of porphyrins on plasmid DNA could be monitored by agarose gel electrophoresis. When circular plasmid DNA is subject to electrophoresis, relatively fast migration will be observed for the intact supercoil form (Form I). If scission occurs on one strand (nicking), the supercoil will relax to generate a slower moving open circular form (Form II). If both strands are cleaved, a linear form (Form III) that migrates between Forms I and II will be generated [37].

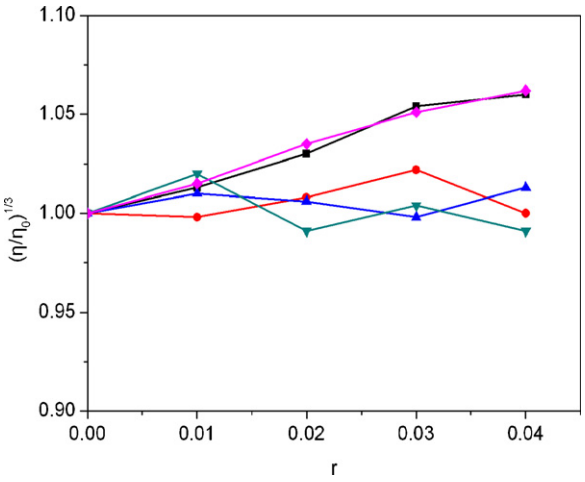

Fig. 8. Plots of the relative viscosity change of CT DNA in the presence of **1** (■), **2** (●), **3** (◆), **4** (▲) and **5** (▼) in buffer A at (30 ± 0.1) °C. [DNA] = 0.5 mM.

In our previous research, porphyrin **1** was proved to employ $^1O_2$ mediated mechanism [19–21] in DNA cleavage, which is a common DNA photocleavage mechanism of porphyrins [38,39]. In order to establish the reactive species responsible for the DNA photocleavage of the metal derivatives of **1**, we investigated the influence of different potentially inhibiting agents. Porphyrin **2** was taken as an example and the result is shown in Fig. 9. Study with NaN_3, a $^1O_2$ quencher [40], was carried out and the cleavage was significantly inhibited (lane 2). The photocleavage efficiency was also greatly inhibited when irradiation reaction was done under an Ar atmosphere (lane 3). On the other hand, the photocleavage ability was enhanced by replacing the reaction media H_2O by 70% D_2O which makes the life span of $^1O_2$ longer (lane 4). These results suggest that $^1O_2$ is likely to be one of the reactive species responsible for the cleavage reaction. Meanwhile, the cleavage of the plasmid DNA was not inhibited in the presence of hydroxyl radical scavengers such as ethanol (lane 5), methanol (lane 6) and DMSO (lane 7) even at high concentration, suggesting that hydroxyl radical may not be the cleaving agent. Similar cases have also been observed for other metalloporphyrins under identical conditions (data not shown), indicating that $^1O_2$ is the reactive species responsible for the cleavage reaction of all these metalloporphyrins.

Because $^1O_2$ was clearly responsible for the DNA photocleavage by the porphyrins in our system, photosensitized productivity of $^1O_2$ was estimated quantitatively by measuring the decomposition of 1,3-diphenylisobenzofuran (DPBF). DPBF directly reacts with $^1O_2$ and subsequently decomposes to 1,2-dibenzoylbenzene. As shown in Fig. 10 for **1** and its metal complexes, absorbance of DPBF (30 mM) at 415 nm linearly decreased in the presence of each porphyrin as illumination time increased. The slopes of the plots of bleached absorption of DPBF versus illumination time are listed in Table 3. The values of the slopes for the metalloporphyrins are larger than the free base porphyrin, indicating that

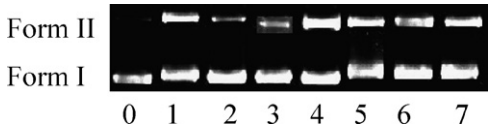

Fig. 9. Photocleavage of pBR322 DNA in the presence of porphyrin **2** and different inhibitors after irradiation by high-pressure mercury lamp for 20 min, in buffer C. 10 μL reaction mixtures contained 1.0 μg of plasmid DNA. [Por] = 1 μM. Lane 0: DNA control; lane 1: in the presence of porphyrin, no inhibitor; lanes 2–6: in the presence of porphyrin and inhibitor, (2) NaN_3 (5 mM), (3) under an Ar atmosphere, (4) 70% D_2O, (5) ethanol (5 mM), (6) methanol (5 mM), and (7) DMSO (5 mM).

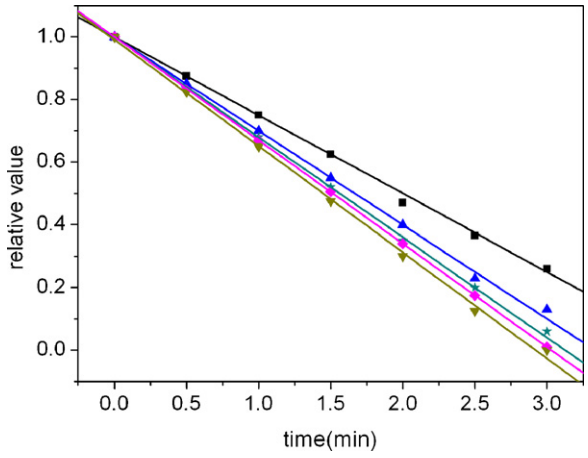

Fig. 10. Decomposition of DPBF by porphyrins **1** (■), **2** (◆), **3** (▲), **4** (▼) and **5** (★). Porphyrin (1 μM) and DPBF (100 μM) were irradiated in pyridine.

Table 3
The slopes (*S*) of the plots of bleached absorption of DPBF by photosensition of porphyrins.

	1	2	3	4	5
S	0.25	0.33	0.29	0.35	0.32

the insertion of metal ions into the cationic porphyrin enhanced the $^1O_2$ productivities effectively. Since it has been reported that the self-aggregation of cationic porphyrins is disadvantageous in $^1O_2$ production [41,42], this enhancement seems to be derived from the increased steric hindrance of metalloporpyrins than free base porphyrin, which could relax the self-aggregation of porphyrin **1**.

Fig. 11 shows the DNA photocleavage results of the porphyrins under identical irradiation by high-pressure lamp. Without irradiation, no substantial cleavage of DNA was observed for all the porphyrins (data not shown). Under comparative experimental conditions, the cleavage abilities of these metalloporphyrins have no obvious difference with the free base porphyrin **1**. Extensive studies have shown that the DNA photocleavage activity of porphyrins is always in parallel with the magnitude of their intrinsic binding constants (K_b) and the DNA intercalators are often more effective in DNA photocleavage than the non-intercalative binders [40,43,44]. The result shown in Fig. 11 is somewhat inconsistent with this experience, since it has been proved above that the metalloporphyrins have lower K_b and more disadvantageous DNA-binding modes than **1**. Nevertheless, it is noteworthy that the experience (the good agreement between DNA photocleavage and K_b) is based an assumption that the compounds have the same $^1O_2$ productivity. Here, the steric hindrance derived from the insertion of metals into porphyrin acts as a "double-edged sword": bring smaller K_b but also higher $^1O_2$ productivity for the metalloporphyrins than the metal-free one. Thus, the DNA photocleavage abilities have no obvious between these metalloporphyrins and their free base porphyrin. The results indicate that both the DNA-

Fig. 11. Photoactivated cleavage of pBR322 DNA in the presence of compounds, light after 20 min irradiation by high-pressure mercury lamp, in buffer C. Lane 0: DNA controlled; lanes 1–5: in the presence of 1 μm porphyrins **1**, **2**, **3**, **4** and **5**, respectively.

binding affinity and the $^1O_2$ productivity are key factors for the DNA photocleavage of porphyrins.

4. Conclusions

Based on absorption, fluorescence, SERS, ICD spectroscopy, thermal denaturation and viscosity measurements, the binding modes of Cu(II)–, Zn(II), Co(III), Mn(III) tricationic metalloporphyrins to CT DNA were investigated in comparison with the free base porphyrin, which is a good DNA intercalator. The intrinsic DNA-binding constants of these tricationic metalloporphyrins are lower than that of free base porphyrin **1**, suggesting that the insertion of metal ions greatly influences the binding of cationic porphyrins to DNA. Among the four metalloporphyrins, only porphyrin **3** intercalates into DNA, while the other three complexes, Zn(II)–, Co(III), Mn(III) porphyrins bind to DNA in non-intercalative mode (outside or groove). This somewhat surprising result may be best understood by the steric hindrance effect that Cu(II) has no axial ligands when coordinating with porphyrin plane while Zn(II)–, Co(III), Mn(III) all have H_2O or Cl on axial position of porphyrin plane. Although have lower K_b, the metalloporphyrin have comparative DNA photocleavage with the free base porphyrin. This could be explained by the higher $^1O_2$ productivities of the metal complexes which also result from the steric hindrance. These results are helpful in better understanding the DNA interactions of cationic porphyrins and may facilitate the design of new anticancer drugs.

Acknowledgements

This work was financially supported by the three following units of the People's Republic of China: the National Natural Science Foundation (29971034, 20071034, 20231010), the N.S.F. of Guangdong Province and Guangzhou Municipality Science &Technology Bureau.

Appendix A. Supplementary data

Supplementary data associated with this article can be found, in the online version, at doi:10.1016/j.saa.2009.12.065.

References

[1] M. Kalek, A.S. Madsen, J. Wengel, J. Am. Chem. Soc. 129 (2007) 9392–9400.
[2] A. Bagno, G. Saielli, J. Am. Chem. Soc. 129 (2007) 11360–11361.
[3] D. Böhme, N. Düpre, D.A. Megger, J. Müller, Inorg. Chem. 46 (2007) 10114–10119.
[4] E. Almaraz, Q.A. Paula, Q. Liu, J.H. Reibenspies, M.Y. Darensbourg, N.P. Farrell, J. Am. Chem. Soc. 130 (2008) 6272–6280.
[5] G.A. Cisneros, L. Perera, R.M. Schaaper, L.C. Pedersen, R.E. London, L.G. Pedersen, T.A. Darden, J. Am. Chem. Soc. 131 (2009) 1550–1556.
[6] L.N. Ji, X.H. Zou, J.G. Liu, Coord. Chem. Rev. 216–217 (2001) 513–536.
[7] F.R. Keene, J.A. Smith, J.G. Collins, Coord. Chem. Rev. 253 (2009) 2021–2035.
[8] A.M. Pizarro, P.J. Sadler, Biochimie 91 (2009) 1198–1211.
[9] E. Fouquet, J. Bernadou, B.J. Meunier, G. Pratviel, Chem. Commun. 15 (1987) 1169–1171.
[10] D.K. Deda, A.F. Uchoa, E. Caritá, M.S. Baptista, H.E. Toma, K. Araki, Int. J. Pharm. 376 (2009) 76–83.
[11] B. Ward, A. Skorobogarty, J.C. Dabrowiak, Biochemistry 25 (1986) 6875–6883.
[12] M. Tabata, K. Nakajima, E. Nyarko, J. Inorg. Biochem. 78 (2000) 383–389.
[13] L. Guo, W.J. Dong, X.F. Tong, C. Dong, S.M. Shuang, Talanta 70 (2006) 630–636.
[14] R.F. Pasternack, P. Garrity, B. Ehrlich, C.B. Davis, E.J. Gibbs, G. Orloff, A. Giartosio, C. Turano, Nucleic Acids Res. 14 (1986) 5919–5931.
[15] R.F. Pasternack, E.J. Gibbs, J.J. Villafranca, Biochemistry 22 (1983) 2406–2414.
[16] L.A. Lipscomb, F.X. Zhou, S.R. Presnell, R.J. Woo, M.E. Peek, R.R. Plaskon, L.D. Williams, Biochemistry 35 (1996) 2818–2823.
[17] M. Tabata, A.K. Sarker, E. Nyarko, J. Inorg. Biochem. 94 (2003) 50–58.
[18] R.K. Wall, A.H. Shelton, L.C. Bonaccorsi, S.A. Bejune, D.R. McMillin, J. Am. Chem. Soc. 123 (2001) 11480–11481.
[19] P. Zhao, L.C. Xu, J.W. Huang, K.C. Zheng, B. Fu, H.C. Yu, L.N. Ji, Biophys. Chem. 135 (2008) 102–109.
[20] P. Zhao, L.C. Xu, J.W. Huang, K.C. Zheng, B. Fu, H.C. Yu, L.N. Ji, Spectrochim. Acta A 71 (2008) 1216–1223.
[21] P. Zhao, L.C. Xu, J.W. Huang, K.C. Zheng, B. Fu, H.C. Yu, L.N. Ji, Biophys. Chem. 134 (2008) 72–83.
[22] P. Zhao, L.C. Xu, J.W. Huang, K.C. Zheng, B. Fu, H.C. Yu, L.N. Ji, Bioorg. Chem. 36 (2008) 278–287.
[23] C. Casas, B. Saint-Jalmes, C. Loup, C.J. Lacey, B. Meunier, J. Org. Chem. 58 (1993) 2913–2917.
[24] M.E. Reichmann, S.A. Rice, C.A. Thomas, P. Doty, J. Am. Chem. Soc. 76 (1954) 3047–3053.
[25] N.T. Sergei, A.G. Victor, S.C. Vladimir, T. Pierre-Yves, J. Raman Spectrosc. 36 (2005) 962–973.
[26] B.C. Baguley, M. Lebret, Biochemistry 23 (1984) 937–943.
[27] J.R. Lakowicz, G. Webber, Biochemistry 12 (1973) 4161–4170.
[28] J.B. Lepecp, C. Paoletti, J. Mol. Biol. 27 (1967) 87–106.
[29] J.D. Groot, R.E. Hester, J. Phys. Chem. 91 (1987) 1693–1696.
[30] C.Y. Wei, G.Q. Jia, J.L. Yuan, Z.C. Feng, C. Li, Biochemistry 45 (2006) 6681–6691.
[31] M. Procházka, P.Y. Turpin, J. Sÿtěpánek, J. Bok, J. Mol. Struct. 482–483 (1999) 221–224.
[32] S.N. Terekhov, S.G. Kruglik, V.L. Malinovskii, V.A. Galievsky, V.S. Chirvony, P.Y. Turpin, J. Raman Spectrosc. 34 (2003) 868–881.
[33] E. Gaudry, J. Aubard, H. Amouri, G. Levi1, C. Cordier, Biopolymers 82 (2006) 399–404.
[34] J. Hanzlıková, M. Procházka, J. Sÿtěpánek, J. Bok, V. Baumruk, P.J. Anzenbacher, J. Raman Spectrosc. 29 (1998) 575–584.
[35] H.T. Daryono, M. Shunsuke, A. Takehiro, Y. Naoki, I. Hidenari, J. Inorg. Biochem. 85 (2001) 219–228.
[36] S. Satyanarayana, J.C. Dabrowiak, J.B. Chaires, Biochemistry 32 (1993) 2573–2584.
[37] J.K. Barton, A.L. Raphael, J. Am. Chem. Soc. 106 (1984) 2466–2468.
[38] T.J. Dougherty, C.J. Gomer, B.W. Henderson, G. Jori, D. Kessel, M. Korbelik, J. Moan, Q. Peng, J. Natl. Cancer Inst. 90 (1998) 889–905.
[39] E.D. Sternberg, D. Dolphin, C. Bruckner, Tetrahedron 54 (1998) 4151–4202.
[40] T. Jia, Z.X. Jiang, K. Wang, Z.Y. Li, Biophys. Chem. 119 (2006) 295–302.
[41] Y. Ishikawa, N. Yamakawa, T. Uno, Bioorg. Med. Chem. 10 (2002) 1953–1960.
[42] N. Yamakawa, Y. Ishikawa, T. Uno, Chem. Pharm. Bull. 49 (2001) 1531–1540.
[43] H. Taima, A. Okubo, N. Yoshioka, H. Inoue, Chem. Eur. J. 12 (2006) 6331–6340.
[44] B. Chen, W. Qin, P. Wang, T. Tian, H.J. Ma, X.P. Cao, X.J. Wu, X. Zhou, X.L. Zhang, F. Liu, F. Zheng, X. Li, Bioorg. Med. Chem. Lett. 13 (2003) 3731–3733.